COMPARATIVE STUDY OF HEAT AND FLUID FLOW CHARACTERISTICS OF PARALLEL AND OFFSET STRIP FIN MICRO-CHANNELS USING CFD SIMULATIONS

by

Vinod K. VENKITESWARAN [a*], ***Cheah C. YEE*** [b], ***and Chia C. MING*** [b]

[a] School of Engineering and Physical Sciences, Heriot-Watt University Malaysia, Putrajaya, Malaysia
[b] Faculty of Engineering and Built Environment, SEGi University, Selangor, Malaysia

Original scientific paper
https://doi.org/10.2298/TSCI171226264V

The primary aim of this study was to consider novel configurations of water-cooled micro-channel layout and compare them with existing configurations. The authors emphasize on establishing a benchmark based on investigations by earlier researchers and numerically analysing them. As a first attempt, offset strip fins are compared with existing parallel fins in terms of subsequent flow fields and temperature profiles. In offset types designated as A and B, the highest velocities occur at the side channels because of the straight wall allowing smooth flow through the channel. Generally, for offset type, the velocity increases after the sidewalls towards the centre. Type A configuration had an uneven velocity profile because of its staggered channel entrance. The lowest average temperature was observed in parallel heat sinks, followed by type A and type B. Causes are discussed for the observed differences and criteria are suggested for the selection of an appropriate geometry of offset fins. An efficient cooling system will ensure effective working of equipment resulting in low energy consumption and better sustainability. This work opens a platform for research on various other configurations and their use in micro-channel cooling.

Key words: *micro-channel, parallel fins, offset strip fins, numerical simulation*

Introduction

The components in an integrated circuit generate heat and cause a significant rise in temperature of the component. With higher heat fluxes, there is more heat generated and there is a need for improved and efficient heat exchangers. This is especially true in electronic applications for the military, where high heat dissipation is critical and need for functioning in harsh environments is mandatory. Even though some manufacturers set design temperatures of electronic components as high as +150 °C (for military applications), it is desirable to keep the surfaces of most components under the +85 °C level for high reliability.

The first study of micro-channels is credited to Tuckerman and Pease [1]. The study then yields a forty-fold improvement in practical compact internal combustion heat-sinking capability marking it as a high performance heat removal system. To study the case of sub-millimeter sized passages, Wang and Peng [2] used small diameter stainless steel tubes with deionized water as the fluid to study the friction factor and Nusselt number. They observed

* Corresponding author; e-mail: v.venkiteswaran@hw.ac.uk

that the Nusselt number was lower than the theoretical value for laminar flow and was dependent on the Reynolds number. In the turbulent regime, the measured Nusselt number was almost 1/3 of the value predicted by Colburn's correlation and the transition to turbulence begins at the critical Reynolds number of 700, which was lower than the standard 2300 for internal flow of conventional flow passages. They also noted that friction factors diverge significantly from the theoretical prediction in the laminar regime. However, Hetsroni *et al.* [3] in their paper comparing the predictions of the theory and experimental data state that the results do not agree with those reported by others (in preceding studies) and are probably incorrect. Peng and Peterson [4] observed an inconsistent pattern in friction factor compared to theory and attributed this behaviour to the early onset to transition to turbulence, which they observed for larger channels at Reynolds number of 400 and smaller channels with Re = 70. Mala and Li [5] showed that the higher pressure gradient measured may be due to early transition to turbulence or surface roughness, which in turn increases the momentum transfer in the boundary-layer near the wall which was confirmed by Qu *et al.* [6]. Qu and Mudawar [7] concluded that the conventional Navier-Stokes and energy equations adequately predict pressure drop and heat transfer of the heat sink.

The definition of *micro-channe*l is still a topic of debate among researchers. Mehendale *et al.* [8] used the following classification based on manufacturing techniques to obtain various ranges of channel dimensions, C_d:

– micro-channels: 1 μm < C_d < 100 μm,
– mini-channels: 100 μm < C_d < 1 mm,
– compact channels: 1 mm < C_d < 6 mm, and
– conventional channels: 6 mm < C_d.

Kandlikar and Grande [9] proposed a different classification based on the Knudsen number to derive the channel hydraulic diameter. The classification is mainly developed for gas flow considerations, but it is also recommended for liquid and two-phase flow applications as well. The following is their proposition classification scheme:

– molecular nano-channels: ≤ 0.1 μm,
– transitional channels: 0.1 μm < ≤ 10 μm,
– transitional nano-channels: 0.1 μm < ≤ 1 μm,
– transitional micro-channels: 1 μm < ≤ 10 μm,
– micro-channels: 10 μm < ≤ 200 μm,
– mini-channels: 200 μm < ≤ 3 mm, and
– conventional channels: > 3 mm.

A simpler classification was proposed by Obot [10] where the hydraulic dimeter is calculated based on the geometry of the channel and proposed that micro-channels were those with hydraulic diameters less than 1 mm (< 1 mm) which were later adopted by many other researchers such as Bahrami and Jovanovich [11], Bahrami *et al.* [12] and Bayraktar and Pidugu [13]. The scheme by Obot [10] is more convenient as it is based on the channel geometry alone and that it utilized the concept of hydraulic diameter, which is the primary representative dimension for internal flow geometry of a heat exchanger.

Lee *et al.* [14] investigated the flow of pressurized nitrogen gas and heat transfer through rectangular micro-channels with a range of width from 194 μm to 534 μm with a Reynolds number range from 300 to 3500. Their results showed that the computational results using ANSYS FLUENT© were in good agreement with the experimental results. Another similar study was conducted by Reynaud *et al.* [15] where they conducted the experiments for mini-channels with a channel thickness of 300 μm to 1.12 mm which was compared with a

simulation with ANSYS FLUENT© and the results were consistent with the conclusions of Lee *et al.* [14]. They attributed minor deviations between the experimental data and CFD results to microscopic effects, such as viscous dissipation and entry effects and imperfections of the experimental apparatus.

Vinodhan and Rajan [16] proposed four geometry configurations different from that of Chien and Chen [17]. The whole geometry used is the same as [17], the differences in geometry was that the plenums of the inlet and outlet were 4.2 × 1 mm and it is divided into quadrants, each with separate inlet and outlet. These new configurations are compared to the conventional I-type heat sink and the results show that the new design has lower maximum and minimum substrate temperature, the lower temperature gradient of the substrate and higher Nusselt number and heat transfer rate. Colgan *et al.* [18] designed a single-phase silicon offset strip micro-channel that consisted of six heat exchanger zones and optimized cooler fin designs. They concluded based on their studies that a silicon micro-channel can be integrated with a single chip module in a simple and practical manner while providing excellent thermal performance.

Kandlikar and Upadhye [19] from their work concluded that the best design would be the offset strip fin configuration in a split flow arrangement. Hong and Cheng [20] found that the best performance is obtained when the fin interval is equal to fin length and more rows of fins require higher mass-flow rate for lower wall temperatures. A few studies are on inlet-outlet configuration, concluding that vertical inlet-outlet arrangements have better flow and heat dissipation [16, 21].

The objectives of this work are:

– to compare the simulated results with results by Chein and Chen [17] for the parallel (I-type) fin configuration by means of fluid-flow and temperature distribution, and
– to contrast the three different fin types (parallel/I-type, type A, type B by means of fluid-flow and temperature distribution and determine which produces the best performance.

Methods

This work involves numerical simulation using a commercial CFD software ANSYS FLUENT© as illustrated below.

Design of micro-channels

A micro-channel heat sink generally consists of a micro-channel base layer, cover plate along with an inlet and outlet. The geometric configuration of the micro-channel heat sink is shown in figs. 1 and 2. The parallel type micro-channel heat sink design by Chein and Chen [17] has been replicated for this study with another two new design configurations replacing the parallel heat sink with an offset strip fin heat sink. The size of the micro-channel heat sink is 6.2 × 18 × 0.5 mm. The heat sink area consists of 11 channels, each channel with dimensions of 200 μm × 400 μm × 10 mm. The wall thickness of the fin is set so that it equals the width of the channel, *i. e.*, $W_c = W_f = 200$ μm. The width of the sidewalls is 1 mm.

The inlet and outlet plenums with width and length of 4.2 mm and 3 mm, respectively, were meant for distributing and collecting fluid-flow into and out of the micro-channel. The inlets and the outlets are located in the centre of the short wall opposing each other with openings of 1.8 mm.

For the offset strip fin design, staggered fins of length, L_f, are spaced at the distance of, L_g. The fins are arranged in rows similar to the parallel micro-channel. The optimal ratio of fin interval to fin length is $L_g/L_f = 1$ [9]. Both offset strip fin configurations have a fixed fin

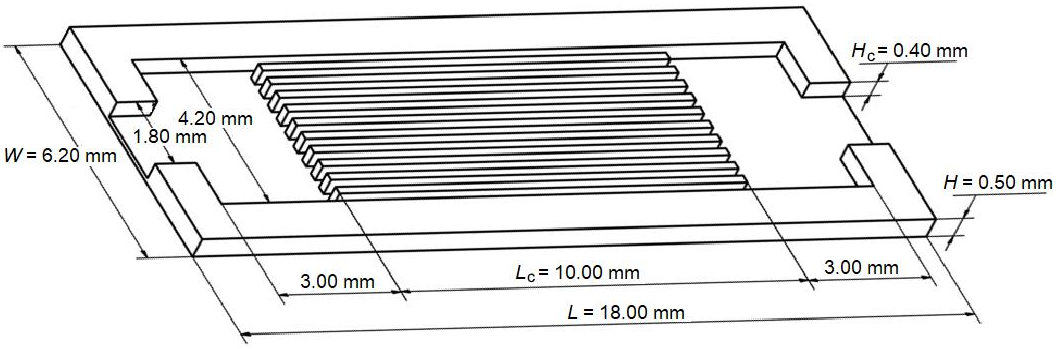

Figure 1. Geometric configuration of parallel type micro-channel heat sink

dimension of 0.5 mm, with 10 units of fins over the whole length of the micro-channel, L_c = 10 mm for the whole heat sink region. For type A, fins in the odd-numbered row (*i. e.* 1, 3, 5, 7, 9) start with half a fin and the even numbered row fins (*i. e.* 2, 4, 6, 8, 10) are staggered by $L_g/2$. For type B, fins in the odd-numbered row (*i. e.* 1, 3, 5, 7, 9) start with the fin of length ¾ L_f and the even numbered row fins (*i. e.* 2, 4, 6, 8, 10) start with a full-length fin. This is depicted in fig. 3.

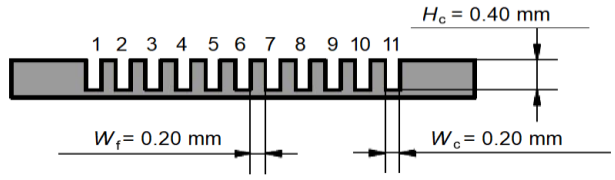

Figure 2. Front view of the micro-channel inlet showing heat sink micro-channel dimensions and channels numbering

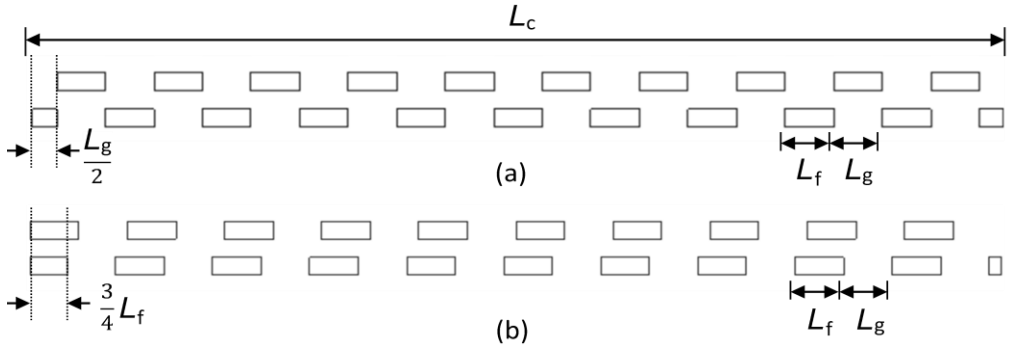

Figure 3. Schematic of fin arrangement; (a) offset strip type A, (b) offset strip type B (the dimensions are fixed where $L_f = L_g$ = 0.5 mm and L_c = 10 mm, the total number of fins/row is 10)

Assumptions made in the analysis

The following assumptions are made in the work:

(1) steady fluid-flow and heat transfer,
(2) incompressible fluid and subsonic flow,
(3) constant solid and fluid properties,
(4) constant heat flux at the base plate, and
(5) heat transfer to air at the cover plate is negligible as compared to heat transfer to water over the fins; hence this surface is assumed to be an insulated surface.

Boundary conditions for flow and heat transfer

The pressure is prescribed at the channel inlet:

$$p(0) = p(\text{prescribed}) \tag{1}$$

At the inlet of the micro-channel, $x = 0$, the velocity is initially specified (a trial velocity) not as a boundary condition, but iteratively corrected until the pressure drop is satisfied.

Outlet boundary condition

Pressure outlet conditions were employed (zero-gauge pressure):

$$P(\text{outlet}) = 0 \tag{2}$$

The outlet velocity boundary condition is based on zero diffusion flux.

In literature, a variety of other boundary conditions have been investigated. A commonly used boundary condition considers:

$$\frac{\partial^2 u}{\partial \eta^2} = 0 \tag{3}$$

η is the outward normal to the outlet plane and at the walls.

At all fluid-solid interfaces, no slip condition is taken:

$$\vec{\mathrm{V}} = 0 \tag{4}$$

The work of Chein and Chen [17] considers a fixed pressure drop across the channel. As this paper compares the results with [17], the same values of fixed pressure drop across the chanel of 25, 35, and 50 kPa are considered.

To ensure that the computed numerical solution satisfies the prescribed pressure drop, the solution algorithm follows this procedure:

With an initial trial inlet velocity, the solution algorithm calculates the pressure at exit. If this pressure is not equal to outlet zero-gauge pressure, an appropriate new trial velocity value at inlet is chosen and iterations of the computation continue until the prescribed pressure at outlet is satisfied. Each inlet velocity corresponds to a particular mass-flow rate and thus, values of mass-flow rates are not prescribed.

The heat transfer calculations consider heat flow in the fin as well as in the coolant flowing in the channel. A conjugate solution approach is used. Boundary conditions required for both conduction in the silicon part, as well as for convection in water are the following:

$$T(0) = T(\text{inlet}) \tag{5}$$

At channel outlet:

$$\frac{\partial^2 T}{\partial \eta^2} = 0 \tag{6}$$

At the base plate, the heat flux is specified:

$$-k_S \frac{\partial T_S}{\partial \eta} = q'' \tag{7a}$$

At the fluid-solid interface, continuity of temperature and heat flow are applied:

$$T(\text{solid}) = T(\text{water}) \tag{7b}$$

$$-k_S \frac{\partial T_S}{\partial \eta} = -k_W \frac{\partial T_W}{\partial \eta} \tag{7c}$$

At the channel cover where heat transfer to air is neglected:

$$\frac{\partial T_S}{\partial \eta} = 0 \tag{7d}$$

Numerical parameters and procedures

The ANSYS FLUENT© was used to run the numerical simulations for the different geometric configurations. A uniform heat flux, q, of 100 W/cm^2 was applied to the base of the heat sink to simulate the heat generated by the chip. The inlet was chosen as pressure-inlet set to the pressure drop across heat sink, Δp = 50 kPa. The inlet water temperature was fixed at 293 K.

Table 1. Grid sensitivity analysis along channel 11 (q = 100 W/cm^2 and pressure drop, Δp = 50 kPa)

Geometry	Number of mesh elements	T_{avg} [K]	Deviation [%]
I-type	337210	329.33	–
	580471	327.74	0.482
	1010883	327.02	0.220
	1243913	326.55	0.144

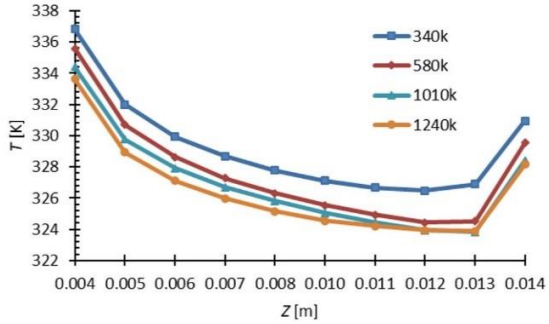

Figure 4. Comparison of substrate surface temperature along channel 11 in parallel heat sink using 4 different number of mesh elements

A grid sensitivity analysis was carried out with the number of mesh elements of 340k, 580k, 1010k, and 1243k for the parallel micro-channel. The substrate surface temperature along channel 11 was recorded. Based on the outcome that 1, elements and 1240k elements were similar, 1010k elements were adopted for this study.

Table 1 shows that the simulation results of the average substrate to fluid surface temperature for channel 11 were almost identical for computation with the number of elements of 1010k and 1240k as the percentage deviation of 0.144%. This is reflected in fig. 4. A higher number of elements would require a greater computational load, which is not necessary since the percentage deviation is so low.

Based on these results, a computational cell with 1010k elements is used throughout the computation in this study.

Table 2. Material properties for solid and fluid

Material	Properties	Value
Silicon	Density, ρ [kgm^{-3}]	2719
	Specific heat, c_p [Jkg^{-1}K^{-1}]	712
	Thermal conductivity, k_s [Wm^{-1}K^{-1}]	148
Water	Density, ρ [kgm^{-3}]	998.2
	Specific heat, c_p [Jkg^{-1}K^{-1}]	4182
	Thermal conductivity, k_{flu} [Wm^{-1}K^{-1}]	0.6
	Viscosity, μ [kgm^{-1}s^{-1}]	$1.003 \cdot 10^{-3}$

The spatial discretization in the momentum, energy, turbulent kinetic energy, and turbulent dissipation rate were solved by the first-order upwind scheme to save on computation time. The coupling of pressure-velocity was solved by setting to a SIMPLE scheme. The convergence criterion for velocity and energy was left at default settings of $1 \cdot 10^{-3}$ and $1 \cdot 10^{-6}$. Solution

initialization methods used was standard initialization computing from the inlet. The material of the heat sink is silicon and the fluid coolant is water. The properties of the materials are listed in tab. 2. The results were analysed by taking data points along the centre of each micro-channel.

Results and discussion

From the various sets of available results only representative ones are presented for the sake of brevity.

Computation comparison

Parallel fin design was first simulated with different pressure drops of Δp = 25 kPa, 35 kPa and 50 kPa, and was computed and compared with the results provided by Chein and Chen [17] as given in fig. 5.

As seen from fig. 5, the computed results yield similar velocities from the results from Chein and Chen [17], for all pressure drop (Δp = 25 kPa, 35 kPa, and 50 kPa), with an average difference of not more than 0.1 m/s. The computed results are only slightly higher with the largest difference of 0.3 m/s at channel 1 and 11.

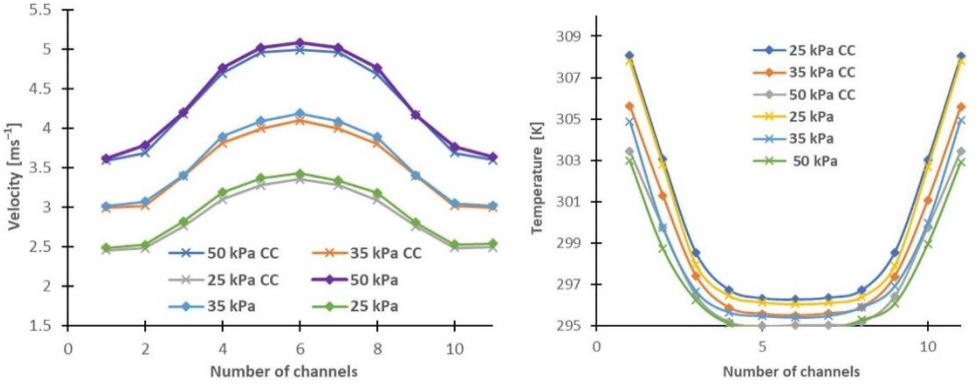

Figure 5. Comparison of computed velocity and temperature for I-type heat sink at different pressure drops of Δp = 25 kPa, 35 kPa and 50 kPa [17]

The computed temperature profiles are somewhat lower than the results of [17]. This could be seen on the channels adjacent to the sidewalls. At a pressure drop of Δp = 25 kPa, the temperature difference is more evident with a maximum temperature difference of approximately 5° and channels 3 to 9 have their values closer with a variance of not more than 1 K. This deviation in results may be due to the different simulation models used. Whereas [17] used a laminar model, this work uses a k-ε turbulence model. With very low values of kinetic turbulent energy and kinetic turbulent dissipation to simulate a laminar flow-based on the studies by Peng *et al.* [22, 23], the laminar flow transition occurred at Reynolds numbers of 200-700, upper bound of the laminar heat transfer regime occurred at a Reynolds number of 200-700 and fully turbulent convective heat transfer was reached at Reynolds numbers of 400-1500.

When compared with the [17] results, the present computed results are reasonably similar. However, no importance is given to this apparent agreement. The main point of interest was to achieve velocity and temperature profiles for the chosen configurations and analyse their flow and thermal behaviour for guidance in the design of the coolant channels.

Flow field

In fig. 6, the flow fields for the three different types of heat sinks studied are shown for Δp = 50 kPa. There exist re-circulation zones at the far corners of the inlet and outlet plenums as reported by Chein and Chen [17] and is to be expected. This is because of the locations of the inlets and outlets where the fluid flows horizontally across the heat sink and can be compared to fluid flow in a cavity [24]. The location of the inlet will significantly affect the average velocities which can be seen for channels 5 to 7 having high average velocities since it is located directly opposite the inlets and outlets which can be seen in fig. 6.

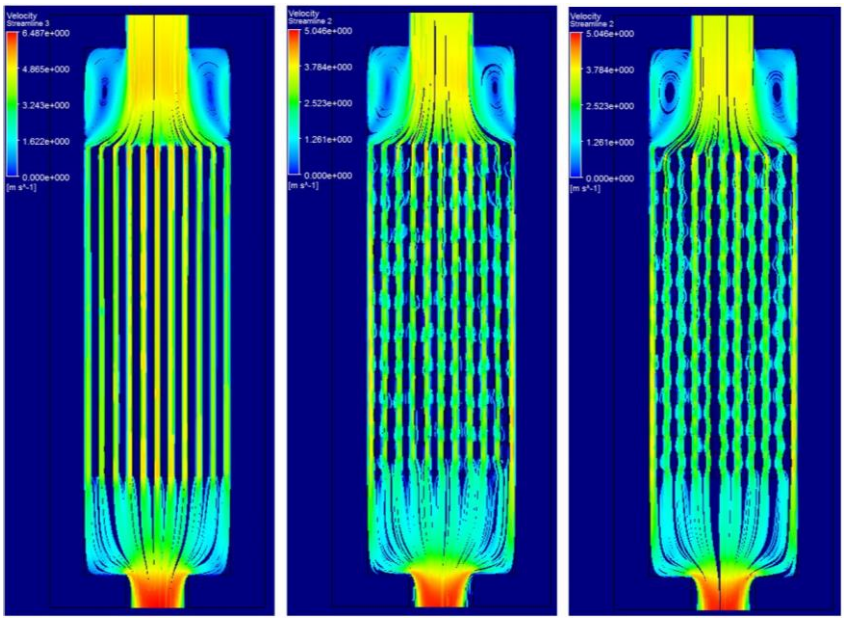

Parallel **Offset type A** **Offset type B**

Figure 6. Flow fields of various micro-channel heat sink configurations, at the mid-plane of the heat sink

Offset strip fins for both type A and B have the highest velocities along the sidewall along channel 1 and 11. From fig. 6 we can see that, as fluid flows through the offset strip fins, the flow path direction changes periodically due to the periodic obstruction of the strip-fins. The periodic change causes large re-circulation of flow around the corners of the strip-fins [20]. This obstruction inhibits the flow of fluid, reducing the average velocities along channels 2 to 10. Along with channels 1 and 11 for both type A and B, this periodic change in direction can also be observed for fluid on the strip-fin side, but not for the flat wall. There is, therefore, less obstruction to flow in the outermost channels, thus giving the highest velocities for both types A and B. The average mass-flow rate and velocity in the three different configurations are given in tab. 3 below.

From tab. 3, it is seen that, for given pressure drop, the maximum velocity and mass-flow rate occur for the parallel channel followed by type B and type A. This evidently reflects the fact that the resistance to flow is least for the parallel plate channel. An examination of the boundary-layer formation on the fin walls reveals some interesting features.

Table 3. Average mass-flow rate and velocity of water of various micro-channel heat sink configurations

Micro-channel heat sink configurations	A type	B type	Parallel
Average mass-flow rate [kgs^{-1}]	219.7342	235.0998	350.4976
Average velocity [ms^{-1}]	2.75	2.95	4.39

In the case of the parallel channel, the flow reaches full development in the fashion of the Hagen-Poiseuille flow between plates. Once the flow is fully developed, the friction factor reaches its lowest value and remains constant.

When the strip fins are staggered, the flow is periodically interrupted. As compared to offset fin type A, the growth of the boundary-layer in the case of offset fin B is closer to that of fully developed flow as shown in fig. 7. In this case, the boundary-layers from adjacent rows tend to converge. This explains the lower flow resistance of type B fins and the higher mass-flow. In design of offset fins, this consideration can be important.

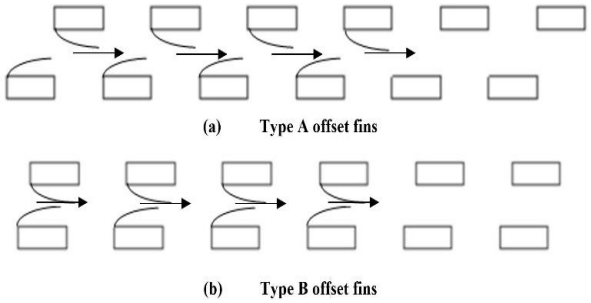

Figure 7. Boundary-layer development for type A and B offset fins

Temperature distribution

Figure 8 shows the temperature distribution for the three different geometries. Fluid- flow is from the top to the bottom as indicated by red arrows. The high temperature regions are located at the corners of the substrate where there is poor heat transfer. The low temperature regions are where the fins are located nearest to the inlet. The reason for this may because of cold fluids flowing in, therefore high heat transfer taking place. In addition, the micro-channel fins have a higher effective surface area for convective heat transfer to occur. Channels that are closer to the sidewalls have higher temperatures, as the heat density at the sidewall is higher and more heat needs to be carried away by the fluid. From fig. 7 significantly high temperature regions are visible, especially at the corners of the inlet and outlet plenums. As water flows, the heat is transferred to the fluid by convection. However, the hot water is not instantly carried towards the outlet, therefore having lower heat transfer capacity. *Dead* zones near the tips of the plenum of the water circulation region are where the temperature is maximum, even though the whole surface is in contact with the fluid. The flow in that area is at its lowest, therefore very little heat is carried away from that region.

The temperature at the base plate where it is bonded to the chip must meet a certain temperature requirement for optimal performance. Figure 9 shows the temperature distribution of the base plate. For all geometries, the maximum temperatures occur at the corners, especially nearer to the outlet. Minimum temperatures occur at the micro-channel entrance area. Based on the results, parallel fins have a better surface uniformity. The wavy local low temperatures are because of the periodic change of direction of the flow path of the fluid through the strip-fins as can be seen in fig. 9.

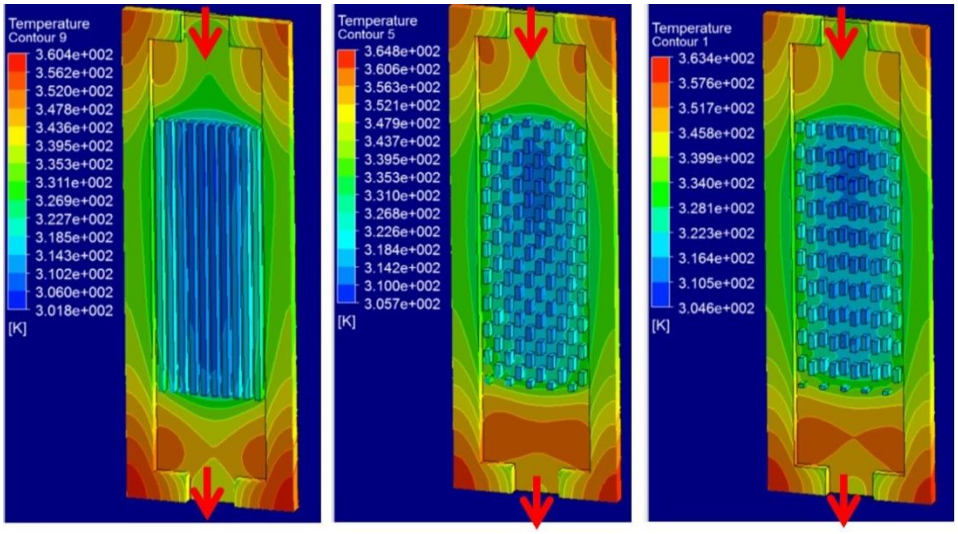

Parallel **Offset type A** **Offset type B**

Figure 8. The temperature distribution of the substrate part of micro-channel heat sinks

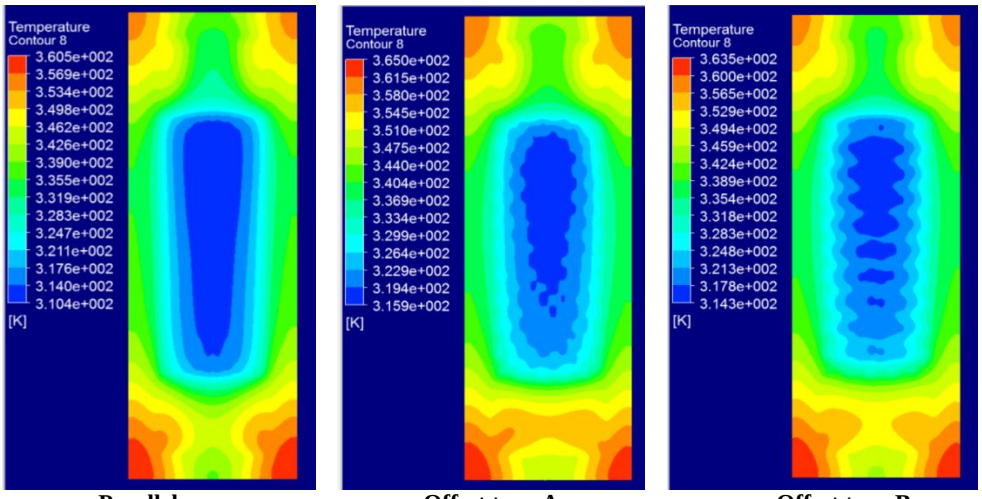

Parallel **Offset type A** **Offset type B**

Figure 9. The temperature distribution of the base plate of the micro-channel heat sinks

Average velocity and temperature for each channel

The average velocities and substrate surface temperatures along each channel for the three different geometries are shown in fig. 10. The substrate surface shown here is the surface in contact with the fluid. In general, the offset strip fins have lower velocities compared to parallel fins. The velocity profiles for parallel and offset type B are symmetrical, which is expected since the inlet of the channelis in a single line. For offset type A the velocity profile is staggered following the staggered geometry of the inlet channels. The velocity dips for cha-

nnels 2, 4, and 9. These channel inlets are indented and have no resistance from incoming flow from the adjacent channel wall. This creates a passageway for the fluid to flow into the next channel, therefore, there is less fluid flowing through these channels.

From fig. 10, the velocity range is within 2 to 5 m/s. The corresponding Reynolds number calculated is from 530 to 1330 based on the hydraulic diameter. This validates the assumption of turbulent flow in the heat sink [22, 23].

For the parallel fin micro-channels, the temperature profile is the inverse of the velocity profile, where the maximum velocities will yield minimum temperatures and *vice versa*. However, for the offset strip-fins, this is not observed. Both offset fins yield a symmetrical temperature profile similar to that of the parallel fin, despite the low velocities along channel 2 to 10. This is due to the periodic change of flow direction around the strip fins as discussed earlier [20]. This periodic change causes re-circulation around the edge of the strip-fin. This local circulation of flow allows the cool fluid at the center of the channel to mix with the hot fluid closer to the fin wall and equalizing the temperatures. The temperature profile for offset type B is slightly better than in type A. This can be attributed to the uniform velocity profile due to the inline channel inlets thus better heat transfer by convection to take place. Based on the results, parallel fins give the better cooling performance followed by offset type B and offset type A.

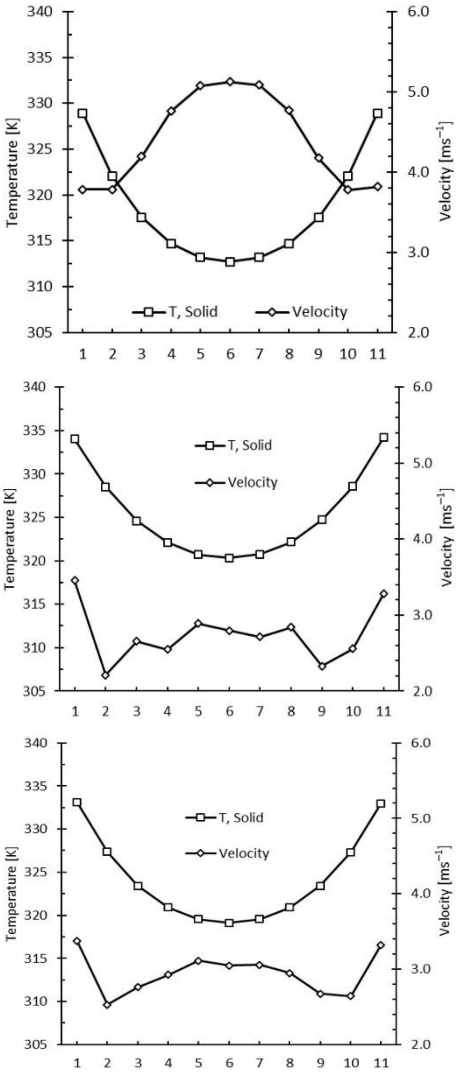

Figure 10. Average velocity profile of fluid and the substrate surface temperature in contact with the fluid for each channel of micro-channel heat sinks of different configuration: (a) parallel, (b) offset type A and (c) offset type B

Conclusions

The numerical analysis of fluid-flow and transfer with a fixed inlet and outlet configuration with three different heat sink configurations was performed in this study. The following inferences can be made based on the simulated results.

- The highest velocity for parallel configuration occurs at the centre of the heat sink because the fluid has a straight flow path from the inlet to the outlet. The lowest velocity is at the sidewalls since it is furthest from the inlet and outlet. In offset types A and B, highest velocities occur at the side channels because of the straight wall allowing smooth flow through the channel. Generally, for offset type, the velocity increases after the sidewalls towards the centre. Type A configuration had an uneven velocity profile because of its staggered channel entrance.

- Higher temperatures were observed at the edge of the heat sink where there is no heat dissipation by convection and re-circulation zones at the inlet and outlet plenums. The lower temperatures occur at the entrance of the micro-channel due to cooler liquid allowing more heat to be absorbed by the fluid, thus higher heat transfer in that region. Temperatures increase along the flow direction because of the constant heat flux from the base plate.
- At a fixed pressure drop across the heat sink, offset type A has the lowest average velocities followed by type B and parallel micro-channels. The offset micro-channels have constant change in flow direction, which inhibits the flow of the fluid.
- The lowest average temperature was observed in parallel heat sinks, followed by types A and type B.

As a conclusion of this study, parallel configuration shows a better heat dissipation across the heat sink for a fixed pressure drop and fixed geometrical inlet and outlet configuration. Thus, it could provide an efficient cooling to the components and can be considered better among the three different micro-channel heat sinks configurations. The offset strip fins employed in this study were limited to two designs and even though the strip fins performed overall poorer than the parallel fins, it is observed that there is a better dissipation of heat at low velocities. Also, the fluid flow orientation used in this study is the low-pressure direction. A research done by Guo *et al.* [25] indicates that fluid low orientation of 45° gives the best thermal-hydraulic performance of fins. Different fin arrangements and geometries can further be studied. The finest option will result in effective working of the equipment resulting in efficient energy consumption and sustainability

Acknowledgment

The authors are obliged to Heriot-Watt University, Malaysia and SEGi University, Malaysia for providing needed facilities and assistance.

Nomenclature

W – width, [mm]
L – length, [mm]
H – height, [mm]

Greek symbols

Δp – pressure drop, [kPa]

Subscripts

c – channel
f – fin
g – gap

References

[1] Tuckerman, D. B., Pease, R. F. W., High-Performance Heat Sinking for VLSI, *IEEE Electron Device Lett.*, *EDL-2* (1981), 5, pp. 126-129
[2] Wang, B., Peng, X., Experimental Investigation on Liquid Forced Convection Heat Transfer through Micro-Channels, *International Journal of Heat and Mass Transfer*, *37* (1994), Supp. 1, pp. 73-82
[3] Hetsroni, G., *et al.*, Fluid Flow in Micro-Channels, *International Journal of Heat and Mass Transfer*, *48* (2005), 10, pp. 1982-1998
[4] Peng, X., Peterson, G., The Effect of Thermo Fluid and Geometrical Parameters on Convection of Liquids through Rectangular Micro-Channels, *International Journal of Heat and Mass Transfer*, *38* (1995), 4, pp. 755-758
[5] Mala, M. G., Li, D., Flow Characteristics of Water in Microtubes, *International Journal of Heat and Fluid Flow*, *20* (1999), 2, pp. 142-148
[6] Qu, W., *et al.*, Pressure-Driven Water Flows in Trapezoidal Silicon Micro-Channels, *International Journal of Heat and Mass Transfer*, *43* (2000), 3, pp. 353-364
[7] Qu, W., Mudawar, I., Experimental and Numerical Study of Pressure Drop and Heat Transfer in a Single-Phase Micro-Channel Heat Sink, *International Journal of Heat and Mass Transfer*, *45* (2002), 12, pp. 2549-2565

[8] Mehendale, S. S., *et al*., Fluid Flow and Heat Transfer at Micro- and Meso-Scales with Application to Heat Exchanger Design, *Applied Mechanics Review*, *53* (2000), 7, pp. 175-193
[9] Kandlikar, S. G., Grande, W. J., Evolution of Micro-channel Flow Passages: Thermohydraulic Performance and Fabrication Technology, *Proceedings*, ASME International Mechanical Engineering Congress and Exposition, Technology and Society and Engineering Business Management, New Orleans, La., USA, 2002, pp. 59-72
[10] Obot, N. T., Towards a Better Understanding of Friction and Heat/Mass Transfer in Micro-channels – A Literature Review, *Microscale Thermophysical Engineering*, *6* (2003), 3, pp. 155-173
[11] Bahrami, M., Jovanovich, M., Pressure Drop of Fully Developed Laminar Flow in Micro-channels of Arbitrary Cross-Section, *Journal of Fluids Engineering*, *128* (2006), 5, pp. 1036-1044
[12] Bahrami, M., *et al*., Pressure Drop of Fully Developed, Laminar Flow in Rough Microtubes, *Journal of Fluids Engineering*, *128* (2006), 3, pp. 632-637
[13] Bayraktar, T., Pidugu, S., Characterization of Liquid Flows in Microfluidic Systems, *International Journal of Heat and Mass Transfer*, *49* (2006), 5-6, pp. 815-824
[14] Lee, P., *et al*., Investigation of Heat Transfer in Rectangular Micro-channels, *International Journal of Heat and Mass Transfer*, *48* (2005), 9, pp. 1688-1704
[15] Reynaud, S., *et al*., Hydrodynamics and Heat Transfer in Two-Dimensional Minichannels, *International Journal of Heat and Mass Transfer*, *48* (2005), 15, pp. 3197-3211
[16] Vinodhan, V. L., Rajan, K., Computational Analysis of New Micro-channel Heat Sink Configurations, *Energy Conversion and Management*, *86* (2014), Oct., pp. 595-604
[17] Chein, R., Chen, J., Numerical Study of the Inlet/Outlet Arrangement Effect on Micro-channel Heat Sink Performance, *International Journal of Thermal Sciences*, *48* (2009), 8, pp. 1627-1638
[18] Colgan, E. G., *et al*., A Practical Implementation of Silicon Micro-channel Coolers for High Power Chips, *IEEE Transactions on Components and Packaging Technologies*, *30* (2007), 2, pp. 218-225
[19] Kandlikar, S. G., Upadhye, H. R., Extending the Heat Flux Limit with Enhanced Micro-Channels in Direct Single Phase Cooling of Computer Chips, *Proceedings*, IEEE 21st Annu. Symp. Semiconductor Thermal Meas. Manag., San Jose, Cal., USA, 2005, pp. 8-15
[20] Hong, F., Cheng, P., Three-Dimensional Numerical Analysis and Optimization of Offset Strip-Fin Micro-channel Heat Sinks, *International Communications in Heat and Mass Transfer*, *36* (2009), 7, pp. 651-656
[21] Lu, M. C., Wang, C. C., Effect of the Inlet Location on the Performance of Parallel-Channel Cold Plate, *IEEE Transactions on Components and Packaging Technologies*, *29* (2006), 1, pp. 30-38
[22] Peng, X. F., *et al*., Frictional Flow Characteristics of Water Flowing through Micro-channels, *Experimental Heat Transfer*, *7* (1994), 4, pp. 249-264
[23] Peng, X. F., *et al*., Heat Transfer Characteristics of Water Flowing through Micro-channels, *Experimental Heat Transfer*, *7* (1994), 4, pp. 265-283
[24] Mendu, S. S., Das, P. K., Fluid Flow in a Cavity Driven by an Oscillating Lid – A Simulation by Lattice Boltzmann Method, *Europea Journal of Mechanics – B/Fluids*, *39* (2013), May-June, pp. 59-70
[25] Guo, X., *et al*., Numerical and Experimental Study of Gas Flows in 2D and 3D Micro-channels, *Journal of Micromechanics and Microengineering*, *18* (2008), 2, pp. 1-8

Paper submitted: December 26, 2017
Paper revised: April 3, 2018
Paper accepted: April 4, 2018